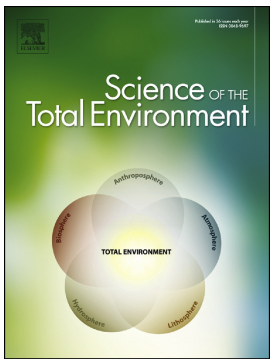

Urban and suburban's airborne magnetic particles accumulated on Tillandsia capillaris

Marcos A.E. Chaparro, Daniela Buitrago Posada, Mauro A.E. Chaparro, Daniela Molinari, Lucas Chiavarino, Brenda Alba, Débora C. Marié, Marcela Natal, Harald N. Böhnel, Marcos Vaira

PII: S0048-9697(23)06517-8

DOI: https://doi.org/10.1016/j.scitotenv.2023.167890

Reference: STOTEN 167890

To appear in: *Science of the Total Environment*

Received date: 14 July 2023

Revised date: 26 September 2023

Accepted date: 15 October 2023

Please cite this article as: M.A.E. Chaparro, D.B. Posada, M.A.E. Chaparro, et al., Urban and suburban's airborne magnetic particles accumulated on Tillandsia capillaris, *Science of the Total Environment* (2023), https://doi.org/10.1016/j.scitotenv.2023.167890

Urban and suburban's airborne magnetic particles accumulated on *Tillandsia capillaris*

Marcos A. E. Chaparro[1,2*], Daniela Buitrago Posada[1], Mauro A. E. Chaparro[3], Daniela Molinari[3], Lucas Chiavarino[1], Brenda Alba[1], Débora C. Marié[1], Marcela Natal[3], Harald N. Böhnel[4], Marcos Vaira[5]

1 Centro de Investigaciones en Física e Ingeniería del Centro de la Provincia de Buenos Aires (CIFICEN), UNCPBA-CICPBA-CONICET, Pinto 399, 7000 Tandil, Argentina.

2 Universidad Nacional del Centro de la Provincia de Buenos Aires (UNCPBA), Facultad de Ciencias Exactas, IFAS, Tandil, Buenos Aires, Argentina.

3 Centro Marplatense de Investigaciones Matemáticas (CEMIM-UNMdP-CICPBA), Universidad Nacional de Mar del Plata (UNMdP), Diagonal J. B. Alberdi 2695, Mar del Plata, Argentina.

4 Centro de Geociencias (CGeo), Universidad Nacional Autónoma de México (UNAM), Boulevard Juriquilla No. 3001, 76230 Querétaro, México.

5 Instituto de Ecorregiones Andinas (INECOA, CONICET), Universidad Nacional de Jujuy (UNJu), Avenida Bolivia 1711, 4600 San Salvador de Jujuy, Argentina

*Name and contact detail of the corresponding author: Marcos A.E. Chaparro. E-mail: chapator@exa.unicen.edu.ar. ORCID ID: 0000-0003-2832-2151. Scopus ID: 26425631300.

Abstract

Air particle pollution is a current issue that can cause adverse problems to human health and the urban environment. A fraction of these emitted particles is magnetite and iron-rich materials, which may be accumulated by biological indicators and effectively characterized by environmental magnetism methods. Thus, we studied this emitted particle fraction using the

epiphytic species *Tillandsia capillaris* growing in northwestern Argentina's urban, suburban, and rural areas. The accumulated airborne magnetic particles' properties revealed valuable information regarding potentially toxic elements, magnetic mineralogy, sizes, morphology, and concentration. Magnetite was detected in samples from all studied areas, and its remanent coercivity values (H_{cr} = 32.1 – 42.6 mT) in (sub)urban sites are similar to other reported cities in Latin America. The concentration of these airborne magnetic particles AMP varied between urban sites (mean and (s.d.) values of *in situ* magnetic susceptibility κ_{is} = 16.2 (9.4) $\times 10^{-6}$ SI, and specific magnetic susceptibility χ = 61.9 (31.4) $\times 10^{-8}$ m^3kg^{-1}) and suburban sites (κ_{is} = 13.9 (9.9) $\times 10^{-6}$ SI, and χ = 43.9 (32.2) $\times 10^{-8}$ m^3kg^{-1}), and it was distinctively higher than in clean sites. The spatial distribution of AMP was analyzed using a geostatistical model for the concentration-dependent magnetic parameter κ_{is}, which showed zones with high magnetic particle accumulation associated with vehicular traffic in the city and industrial emission in a suburban site. Among concentration-dependent magnetic parameters, the κ_{is} is recommended for magnetic biomonitoring because *Tillandsia* species' individuals are not processed for laboratory measurements, preserving them and allowing us the possibility of measurements over time.

Keywords: biomonitor; geostatistical methods; magnetic biomonitoring; magnetite; particle pollution

1. Introduction

Air particle pollution is an increasing concern in cities because of the influence of different anthropogenic activities, i.e., the daily activities of the inhabitants (e.g., vehicular traffic) and external activities (e.g., industrial processes), since they emit dangerous particles into the atmosphere. Emissions from vehicles with internal combustion engines are particularly interesting in all cities since they contribute much particulate matter (PM) from private and

public transportation (Karagulian et al., 2015). Many of these products from vehicular traffic contain fine (< 0.1 – 2 μm) and ultrafine (< 0.1 μm) particles (Palmgren et al., 2003; Nyirő-Kósa et al., 2022). Identifying and quantifying these respirable particles, which may be incorporated into the body and dangerously affect health in urban habitats (WHO, 2021), appears vital. Among the main adverse consequences of (ultra-) fine particles are respiratory tract disorders (such as asthma, chronic obstructive pulmonary disease, acute respiratory infection ARI, and respiratory allergies), headache, irritability, character changes, partial amnesia, cardiovascular problems, possible mental disorders, as well as carcinogenic consequences (Brauer et al., 2002; Pope & Dockery, 2006; Song et al., 2019). According to Muxworthy et al. (2022), the ultrafine magnetic fraction of PM has been underestimated in several works. Their study of air filters from London (UK) showed that the total concentration of ultrafine magnetite particles was 7.5%, significantly higher than previously reported. These ultrafine magnetite particles are capable of causing irreversible damage to vital organs, such as the heart, by causing cell damage (Calderón-Garcidueñas et al., 2019). Kletetschka et al. (2021) point out that these magnetite nanoparticles in the human brain can be associated with diseases such as Alzheimer's.

Since the 2000s, magnetic biomonitoring studies have been reported using plant species in urban and industrial areas. It is possible to use different biological indicators or biomonitors of pollution, such as mosses (Salo et al., 2012; Vuković et al., 2015), lichens (Chaparro et al., 2013; Winkler et al., 2020), *Tillandsia* spp. (Castañeda Miranda et al., 2016; Mejia-Echeverry et al., 2018), leaves and tree bark (Lehndorff et al., 2006; Chaparro et al., 2020). The marked contrast in magnetic composition between airborne magnetic particles (AMP) and plant tissues provides clear advantages for magnetic biomonitoring. This methodology also provides a low-cost alternative in urban sites for establishing an environmental monitoring network of AMP.

Magnetic biomonitoring allows for establishing a monitoring network of air particle pollution at a low cost, taking advantage of natural resources in cities and their surroundings. The exposure time of biomonitor transplants can be established, and the contents of magnetic particles on transplants can be approached with *in situ* magnetic susceptibility measurements (Chaparro, 2021). *In situ* magnetic biomonitoring preserves species and allows the monitoring of magnetic particles over time, a methodology proposed by Marié et al. (2018) and improved by Chaparro (2021).

Among PM and other compounds, airborne magnetite is ubiquitous in cities because of vehicular emissions and, possibly, due to industrial ones. This work hypothesizes that *in situ* magnetic susceptibility measurements may adequately estimate this magnetite accumulated in urban biological indicators. Therefore, this study aims at the following objectives: a) to determine the usefulness of native *Tillandsia capillaris* for magnetic biomonitoring in an urban and suburban area of northwestern Argentina; b) to determine the magnetic, compositional, and morphological properties of particles accumulated in the plant tissues; c) to quantify the contents of AMP in *Tillandsia* sp. tissues using a simple and cost-effective magnetic method, and d) to identify the most impacted areas by AMP pollution in urban and suburban sites in the studied cities.

2 Methods

2.1. Study area and species sampling

The study area is located in San Salvador de Jujuy city and its surroundings, the province's capital, at 1259 m a.s.l, and Palpalá city at 1130 m a.s.l., pinpointed in northwestern Argentina (Fig. 1a). Both cities are placed in a mountainous relief conditioned by the surrounding mountain ranges. The growth of the two localities, which tends to unite, is done around the road axes and the main river that connects them. Their sprawl is partly conditioned by the mountainous context

in which they are located. The current urban sprawl coincides with minor slope areas on the terraces of the Grande River, but in some areas, it has started to invade the slopes of the mountains. The area (Departamento Dr. Manuel Belgrano and Departamento Palpalá) has a population of around 378,400 inhabitants (Censo nacional de población, hogares y viviendas, 2022).

The climate is characterized as subtropical with dry seasons (winter). Summers are warm and rainy (Torres & Pereira, 2018). For 1991–2020 (Servicio Meteorológico Nacional, 2023), annual precipitations reached a mean of 716 mm yr^{-1}, and the annual minimum and maximum temperatures ranged between 6–19°C and 20–31°C, respectively (Fig. S1, Supplementary Material).

Based on reported magnetic biomonitoring studies in Latin America (Castañeda-Miranda et al., 2016; Mejía-Echeverry et al., 2018) and the abundance of *Tillandsia* spp. in the study area, individuals of *Tillandsia capillaris* (Fig. 1b) with similar size (≈ 5 cm in diameter) were collected in March 2022 in the urban areas (sites SS, San Salvador de Jujuy, n = 24, Fig. 1c), the suburban areas (sites J, Jujuy and Palpalá, and RB, Río Blanco, n = 7), and "clean" areas (sites O, PP and TIL, i.e., Finca El Obispo, Planta Potabilizadora Reyes, and Tilquiza, respectively, n = 6) far away from downtown. Individuals of *T. capillaris* living on urban trees were collected from a minimum height of 1.5 – 2 m to avoid the influence of re-suspended soil particles. Each sample was put in a paper bag and stored. First, *in situ* magnetic susceptibility measurements were done on fresh individuals. Since these *in situ* measurements on biomonitors offer a valued and time-saving methodology for biomonitoring magnetic particles simply and effectively (Chaparro, 2021), this new methodology was performed on collected individuals and complemented with routine measurements of environmental magnetism. After that, each plant of

T. capillaris was dried at 38°C for 24 hr. in an electronically controlled oven. About 0.7 g of crushed material was firmly pressed and placed into plastic containers of 8 cm^3 for routine magnetic measurements at the laboratory. In addition, two samples of dust deposited on roofs were collected for comparison purposes, one sample (P-T) at Palpalá and another (P-A) at San Salvador de Jujuy (downtown).

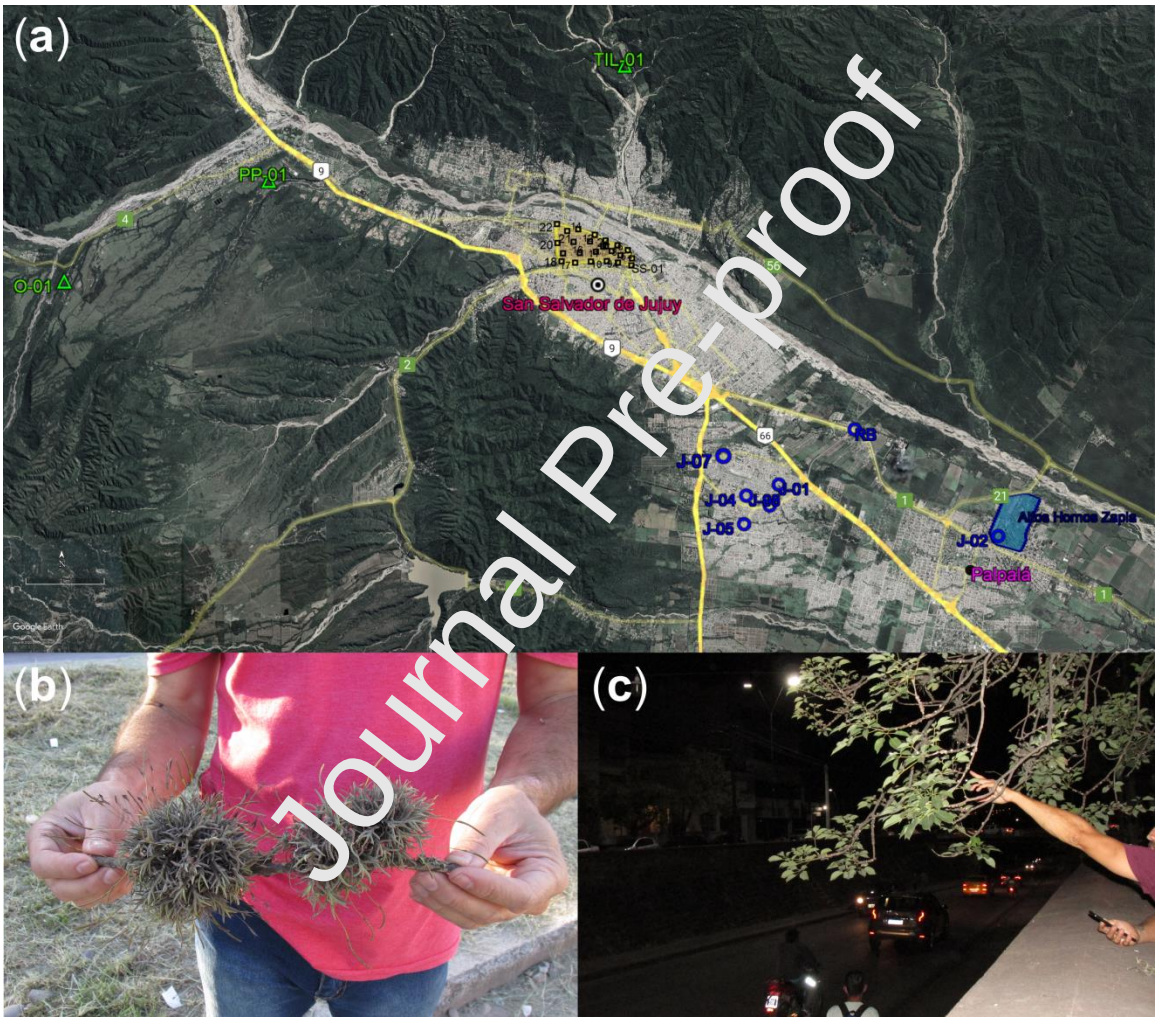

Fig. 1. Sampling sites in northwestern Argentina. (**a**) San Salvador de Jujuy (urban sites SS, 24° 11.624'S; 65° 18.041'W), Alto Comedero, Río Blanco, and Palpalá (suburban sites J and RB) and clean areas (sites O, PP, and TIL). (**b**) Individuals of *Tillandsia capillaris*; (**c**) Collection of samples in urban sites SS.

2.2. In situ magnetic biomonitoring

In situ magnetic susceptibility (κ_{is}) measurements were done using an SM 30 high-resolution range portable meter (ZH Instruments Ltd., Czech Republic), which works at an operating frequency of 8 kHz and has a measurement sensitivity of 1×10^{-7}SI. Ten (n = 10) readings were performed using the protocol proposed by Chaparro (2021) and Buitrago Posada & Chaparro (2022). Corrected values of κ_{is} were averaged, obtaining a representative value with low dispersion similar to the instrument sensitivity. The mentioned protocol allows measuring κ_{is} on species to quantify (sub) micron-sized magnetite particles. The AMP content is quantified using the magnetite's calibration line proposed by Chaparro (2021),

$$Contents\ of\ AMP = 0.1 \cdot \frac{\kappa_{is}}{2.075 \pm 0.007} \quad (1)$$

where *Contents of AMP* are in mg and κ_{is} in 10^{-6} SI units.

Also important, this methodology preserves species, allowing repeat measurements of exposed individuals over time. Since lichen's thallus measured by Chaparro (2021) are flat, κ_{is} measurements were performed by direct contact between the thallus and the portable meter (DCM). Because *Tillandsia capillaris* has a spheroidal shape (Fig. 1b), two measuring methodologies were proposed and tested by Buitrago Posada & Chaparro (2022), i.e., i) measurements by DCM: direct contact between the plant and the meter, and ii) measurements by contact between the portable meter and a Petri plastic dish where the plant is pressed with a block of wood to increase the plant's surface contact and also increase the mass which is effectively measured (PWM, Fig. 2). The PWM methodology was used in this work because PWM (s.d. = 0.4 $x10^{-7}$ – 1 $x10^{-6}$SI, Buitrago Posada & Chaparro, 2022) evidenced low dispersion results comparable to the instrument sensitivity (1 $x10^{-7}$ SI). Caution is recommended

when measuring outdoors because thermal drift may affect κ_{is} readings, e.g., breeze and airflow must be avoided. Although each individual may be measured in the laboratory (Fig. 2a) and re-located to its exposure site, it is possible to reduce the plant's stress if the κ_{is} readings are performed in a closed environment, e.g., inside a car, as shown in Figure 2b, near each exposure site.

Fig. 2. *In situ* magnetic susceptibility measurements (κ_{is}) using the protocol proposed by Chaparro (2021) and Buitrago Posada & Chaparro (2022). Ten readings were performed by contact between a high-resolution range portable meter SM 30 (ZH Instruments Ltd.) and a Petri plastic dish where the plant is pressed with a block of wood to increase the plant's surface contact (PWM). κ_{is} readings at the laboratory (**a**) and inside a car (**b**) close to the sampling site.

2.3. Magnetic measurements

In the Laboratory of Environmental Magnetism at the CIFICEN (UNCPBA, Tandil, Argentina), mass-specific magnetic susceptibility (χ) was measured at an operating field and frequency of 80

A m^{-1}, 0.992 and 16.032 kHz, respectively. Percentage frequency-dependent magnetic susceptibility $X_{FN(1,16)}$ (= (100 × ($\chi_{0.992kHz}$ − $\chi_{16.032kHz}$) / $\chi_{0.992kHz}$) / (ln 16032 – ln 992)) and $X_{FB(1,16)}$ (= ln 10 × $X_{FN(1,16)}$) (Hrouda, 2011) were determined at the two detailed operating frequencies, using an SM-150 L/H magnetic susceptibility meter (ZH Instruments Ltd., Czech Republic). The parameter $X_{FB(1,16)}$ was calculated for comparison purposes with the well-known parameter χ_{FD}% (= 100% × ($\chi_{0.465kHz}$ − $\chi_{4.65kHz}$) / $\chi_{0.465kHz}$). Anhysteretic and isothermal remanent magnetization (ARM and IRM, respectively) were imparted to samples using: i) a partial ARM device coupled with an alternating field (AF) demagnetizer (Molspin Ltd., England), superposing a DC bias field of 50 and 90 μT to a peak AF of 100 mT, and ii) an ASC Scientific Pulse Magnetizer (Narragansett, USA) model IM-10-30, in steps exposing samples to acquisition- and back-fields from 1.7 – 2470 mT. The remanent magnetizations were measured using a JR-6 spinner magnetometer (AGICO Inc., Czech Republic). Among parameters and ratios, mass-specific anhysteretic susceptibility (χ_{ARM}, calculated using linear regression for ARM acquired at DC bias fields of 50 and 90 μT), anhysteretic ratio χ_{ARM}/χ, saturation of IRM (SIRM = IRM_{2470mT}), remanent coercivity (H_{cr}, which is the required back-field to remove the SIRM, or SIRM = 0), S-ratio (= -IRM_{-300mT} / SIRM, where IRM_{-300mT} is the acquired IRM at a back-field of 300 mT), HIRM (= 0.5 * [SIRM + IRM_{-300mT}]) and L-ratio (= [SIRM + IRM_{-300mT}] / [SIRM + IRM_{-100mT}]) were measured and calculated. Magnetic hysteresis measurements were done at the CGeo (UNAM, Querétaro, México) using a MicroMag^{TM} 2900 magnetometer (Alternating Gradient Magnetometer, Princeton Measurements Corporation, USA). The ratios of remanent saturation to saturation magnetization (M_{rs}/M_s) and remanent coercivity to coercivity field (H_{cr}/H_c) were also determined. The temperature dependence of high-field magnetization (magnetic field of 0.5 T), i.e., M-T thermomagnetic measurements, was measured using a

laboratory-made horizontal magnetic translation balance (Escalante & Böhnel, 2011). About 100 mg of bulk material was placed in a special container for detailed thermomagnetic measurements. These measurements were performed in the air, heating samples up to a temperature of 720°C (heating run) and then cooling to room temperature (RT, cooling run) with a controlled heating/cooling rate of 30°C min^{-1}. The temperature was controlled, and the force exerted by the gradient field of the magnet on the sample was compensated and recorded with a sensor that generated an output voltage. Such voltage is recorded using a PicoLog® recorder.

2.4. Microscopy observations

Trapped airborne magnetic particles were observed and examined by scanning electron microscopy using a Phillips microscope model XL30. This microscope also allowed us to analyze the elemental composition of single particles by X-ray energy dispersive spectroscopy with an EDAX model DX4 (detection limit 0.5%).

2.5. Statistical analysis

Descriptive statistics and correlation analysis between magnetic parameters were conducted. A nonparametric one-way analysis of variance, the Kruskal-Wallis test (Conover, 1999), was performed to determine significant (at the 0.05 level) differences between the site's magnetic parameters medians. An exploratory analysis of κ_{is} data was carried out to construct geostatistical models, analyzing the existence of spatial autocorrelation with the Moran Global Index. An Ordinary Kriging was performed to construct prediction maps. It is the most popular interpolation spatial method because it considers knowledge of the spatial variation as represented in the variogram function and does not require additional information than the measurement values and their geographical coordinates. All statistical and multivariate analyses were performed using the R free software (R Core Team, 2022).

3. Results

Magnetic measurements of natives *Tillandsia capillaris* collected from the urban, suburban, and clean sites from the Jujuy area are detailed in Table 1.

Table 1. Magnetic measurements of *Tillandsia capillaris* samples from the study area (Jujuy, NW Argentina).

Sample	**κ_{is}**	**χ**	**χ_{ARM}**	**ARM**	**SIRM**	**HIRM**	**$\chi_{ARM(1,16)}$**	**χ_{ARM}/χ**	**ARM/SIRM**	**SIRM/χ**	**H_{cr}**	**S-ratio**	**L-ratio**
	10^{-6} SI	10^{-8} m^3kg^{-1}	10^{-8} m^3kg^{-1}	10^{-3} Am^2kg^{-1}	10^{-3} Am^2kg^{-1}	10^{-3} Am^2kg^{-1}	%			kA/m	mT		
Urban sites: San Salvador de Jujuy													
SS-1	15.9	50.4	111.5	89.1	3.8	0.03	2.8	2.2	0.024	7.5	37.0	0.98	0.05
SS-2	8.7	38.3	96.9	77.7	2.9	0.00	5.2	2.5	0.026	7.7	37.7	1.00	0.00
SS-3	10.7	27.9	91.6	76.4	2.3	0.0	8.7	3.3	0.033	8.3	3	1.	0.

						0					9.9	00	00
SS-4	40.4	137.8	185.2	146.8	9.0	0.40	0.9	1.3	0.016	6.5	38.9	0.91	0.22
SS-5	16.1	46.1	117.3	88.7	3.5	0.05	2.7	2.5	0.025	7.6	36.0	0.97	0.08
SS-6	9.3	76.6	153.3	125.1	6.1	0.14	2.3	2.0	0.021	7.9	38.1	0.95	0.13
SS-7	8.6	27.4	72.7	59.6	2.3	0.09	2.5	2.7	0.025	8.5	38.3	0.93	0.21
SS-8	17.5	46.6	97.5	80.3	3.7	0.10	2.8	2.1	0.022	7.9	37.3	0.95	0.14
SS-9	21.3	94.8	139.5	117.1	5.9	0.04	2.4	1.5	0.020	6.2	41.7	0.99	0.03
SS-10	13.5	72.9	128.2	96.4	4.2	0.05	1.6	1.8	0.023	5.7	39.6	0.98	0.06

SS-11	12.7	43.9	101.9	83.8	3.5	0.04	6.8	2.3	0.024	7.9	36.0	0.97	0.08
SS-12	5.5	44.1	101.7	83.5	3.1	0.00	4.1	2.3	0.027	7.0	40.5	1.00	0.00
SS-13	14.9	--	--	--	--	--	--	--	--	--	--	--	--
SS-14	20.4	84.1	157.1	140.0	7.4	0.14	2.5	1.9	0.019	8.7	38.5	0.96	0.11
SS-15	9.8	20.5	43.4	32.8	1.5	0.07	3.9	2.1	0.021	7.6	39.9	0.91	0.23
SS-16	17.3	57.4	104.3	87.6	3.6	0.00	3.5	1.8	0.025	6.2	36.7	1.00	0.01
SS-17	13.9	68.3	146.0	120.3	4.7	0.00	8.1	2.1	0.025	6.9	36.5	1.00	0.00
SS-18	15.5	39.2	76.2	65.7	2.6	0.00	6.0	1.9	0.026	6.5	40.5	1.00	0.00
SS-19	42.4	143.2	219.6	161.1	9.6	0.5	2.4	1.5	0.017	6.7	4	0.	0.

						0					2.6	90	25
SS-20	17.4	67.2	129.7	111.6	4.3	0.00	4.2	1.9	0.026	6.4	39.5	1.00	0.00
SS-21	27.0	72.6	128.6	101.4	4.4	0.02	3.3	1.8	0.023	6.1	37.4	0.99	0.02
SS-22	19.0	69.1	122.3	98.9	4.2	0.00	2.8	1.8	0.024	6.1	40.3	1.00	0.00
SS-23	2.8	34.7	103.8	83.7	3.2	0.08	11.9	3.1	0.030	9.1	38.4	0.95	0.15
SS-24	8.9	61.1	211.1	162.0	6.8	0.25	3.7	3.5	0.024	11.2	34.7	0.93	0.20
Suburban sites: Alto Comedero & Palpalá													
RB	7.6	7.9	37.0	27.7	1.1	0.00	6.9	4.7	0.025	13.8	35.7	1.00	0.00
J-01	7.9	49.1	134.6	114.8	4.7	0.2	3.0	2.7	0.024	9.6	3	0.	0.

						2					8.8	91	22
J-02	32.6	110.8	133.6	109.9	9.3	0.00	0.3	1.2	0.012	8.4	38.5	1.00	0.00
J-04	4.8	32.3	96.7	92.9	2.8	0.00	4.9	3.0	0.033	8.7	32.1	1.00	0.00
J-05	13.7	35.0	104.5	93.1	3.2	0.00	3.5	3.0	0.029	9.1	35.7	1.00	0.01
J-07	8.9	29.7	105.3	76.8	3.5	0.21	2.7	3.5	0.022	11.9	36.2	0.88	0.33
J-08	21.6	42.2	111.5	103.9	4.1	0.04	2.9	2.6	0.025	9.7	35.7	0.98	0.06
Clean sites													--
O-01	1.7	5.9	33.7	31.1	1.0	0.10	5.8	5.7	0.031	17.2	42.2	0.80	0.40
O-02	1.5	5.3	36.1	36.1	1.1	0.09	3.1	6.9	0.032	21.5	41.	0.84	0.33

											0		
PP-01	2.3	5.3	64.0	50.9	1.9	0.03	6.4	12.1	0.027	35.9	34.8	0.97	0.08
PP-02	1.7	22.5	113.1	110.7	3.5	0.13	11.6	5.0	0.032	15.4	35.9	0.92	0.21
TIL-01	2.0	11.2	40.6	41.3	1.3	0.05	3.2	3.6	0.031	12.1	34.9	0.93	0.20
TIL-02	2.8	15.1	59.2	63.4	2.2	0.11	4.4	3.9	0.029	14.4	35.9	0.89	0.30

3.1. Magnetic mineralogy

The magnetic properties of accumulated AMP on tissues of *T. capillaris* evidence a dominant ferrimagnetic phase that reached their saturation IRM at fields < 300 mT and the S-ratio values varied between 0.90 – 1 (for urban sites), 0.88 – 1 (for suburban sites), and 0.80 – 0.97 (for clean areas, see Table S1, Supplementary Material). A very low contribution of a high-coercivity phase is observed through the IRM acquisition curves, and the HIRM, i.e., mean and (s.d.) values of HIRM were 0.09 (0.13) $\times 10^{-3}$ m^3kg^{-1} for urban, and 0.07 (0.10) $\times 10^{-3}$ m^3kg^{-1} for suburban sites (Table S1, Supplementary Material). Since HIRM is significantly ($p < 0.01$) correlated with L-ratio ($R = 0.79$ for urban sites and $R = 0.97$ for suburban sites), the HIRM may not provide quantitative information on the absolute concentration of high-coercivity minerals (Liu et al.,

2007) for this study. The H_{cr} values for all sites, i.e., H_{cr} = 32.1 – 42.6 mT, correspond to magnetite-like minerals as reported in the literature, e.g., Peters & Dekkers (2003). Thermomagnetic measurements shown in Figure 3 confirm that magnetite was present through its characteristic Curie temperature of 580 °C. For heating runs, most samples showed a constant decrease in magnetization with temperatures up to 520 °C. A different behavior was observed for samples J-07, SS-22, SS-19, and J-01, where a magnetization increase from ≈ 420 – 560 °C is observed. After the cooling runs, new formation of magnetic minerals was observed through $1 < M/M_{RT} \leq 2$ for samples with the highest concentration-dependent magnetic parameters (SS-4 and J-02) and the lowest ones (O-01, O-02, and PP-01, Fig. 3). Moderate to high values of M/M_{RT} = 2 – 7, indicating a higher neoformation of magnetic minerals, were observed for both urban (SS-10, SS-16, SS-19, SS-20, and SS-22) and suburban (J-01 and J-07) samples.

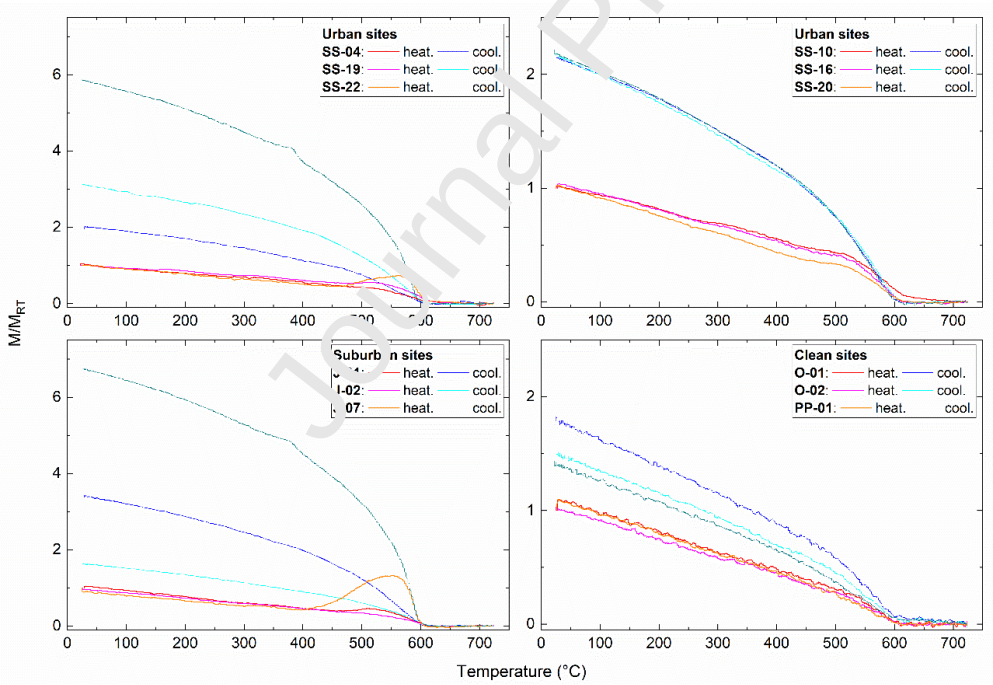

Fig. 3. Thermomagnetic measurements of *Tillandsia capillaris* samples from the Jujuy area (urban sites SS, suburban sites J, and clean sites O and PP). Magnetization (M) was normalized by magnetization at room temperature (M_{RT}); its changes with temperature were recorded for

heating (heat.) and cooling (cool.) runs.

The grain size-sensitive magnetic parameters and ratios, $X_{FB(1,16)}$, χ_{ARM}/χ, SIRM/χ, and ARM/SIRM, showed differences between (sub)urban and clean sites (Table S1, Supplementary Material). Mean and (s.d.) values of $X_{FB(1,16)}$ were 4.1 (2.6)% for urban and 3.5 (2.1)% for suburban sites, indicating a minimum contribution of superparamagnetic (SP) particles (Dearing, 1999). However, the contribution of SP particles seems important for clean sites O and PP, where mean and (s.d.) values of $X_{FB(1,16)}$ were 4.5 (1.9)% and 9.0 (3.7)%. In addition, the mean values of χ_{ARM}/χ, SIRM/χ, and ARM/SIRM are lower for (sub)urban than clean sites, which indicates coarser magnetic particles in the city and surroundings. The magnetic grain size estimation of accumulated AMP was below 5 μm, as shown in Figure 4a. Samples from urban and suburban sites had coarser particles than clean sites, with values falling between 1 – 5 μm, 0.2 – 1 μm, and 0.1 – 0.2 μm (Fig. 4b), respectively. The Kruskal-Wallis test showed significant differences at the 0.05 level between sites (urban–suburban, urban–clean, and suburban–clean) through median values of particle size-dependent magnetic parameters, i.e., χ_{ARM}/χ, ARM/SIRM (only between urban–clean sites), and SIRM/χ (Table S2, Supplementary Material). Among suburban sites, *T. capillaris* (J-02) and dust (P-T) samples from the Palpalá site had coarser particles of 5 μm (Figure 4a), which was expected from its industrial activity developed in the area of the sampling. The ratios M_{rs}/M_s and H_{cr}/H_c from magnetic hysteresis measurements are displayed in the modified Day's plot (Figure 4c). Samples are located in the regions of magnetite's pseudo-single domain (PSD) and the SP + PSD. The SS samples tend to the right, an SP + PSD region (Dunlop, 2002). Mixtures of magnetite were more evident for urban samples SS than others from the mixing curves for single domain size (SD) + multidomain (MD) and the

mixing curves for SP + PSD (Figure 4c). Two magnetic hysteresis loops of urban (SS-10) and suburban (J-02) sites are shown in Figure 4d.

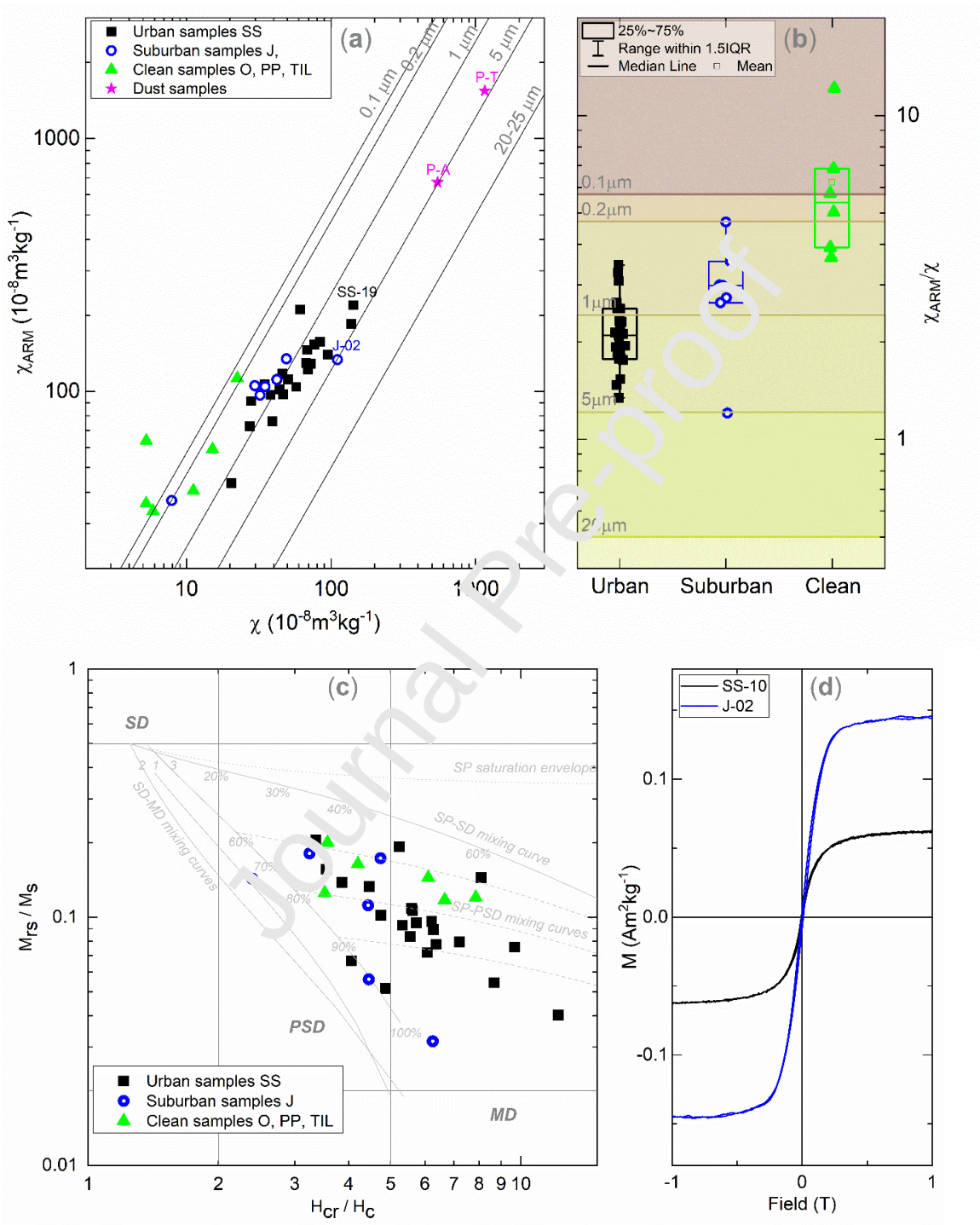

Fig. 4. Particle size-dependent magnetic parameters of AMP on *Tillandsia capillaris* and (urban

sites SS, suburban sites J and RB, and clean sites O, PP, and TIL) and dust samples (P-A at downtown sites SS, and P-T at Palpalá): (**a**) parameters χ_{ARM} and χ are represented, the indicated samples SS-19 and J-02 were observed by SEM-EDS; (**b**) the anhysteretic ratio χ_{ARM}/χ, calibration lines are based on data reported by King et al. (1982); (**c**) parameters from magnetic hysteresis measurements, i.e., M_{rs}/M_s and H_{cr}/H_c, and mixing lines for SD-MD, SD-SP, and SP-PSD (Dunlop, 2002); and (**d**) magnetic hysteresis measurements of samples SS-10 and J-02 are also represented.

3.2. Morphology and elemental composition

Samples SS-19 (urban site) and J-02 (suburban site) were observed by SEM-EDS to analyze the particle's morphology and elemental composition. Ferrimagnetic and fine AMP comprised (sub)micron-sized magnetites accumulated on tissues of *Tillandsia capillaris*, as observed in Figure 5a. These images show *T. capillaris* leaves where shiny Fe-rich particles are spread on flat trichomes of about 200 μm diameter (Fig. 5b). The observed particles in urban (Fig. 5c and 5d) and suburban (Fig. 5e and 5f) sites were irregular and spherical. The mean (s.d.) sizes of trapped Fe-rich particles were 1.3 (0.8) μm for SS-19 and 2.4 (2.3) μm for J-02, which agree with magnetic estimation (Fig. 4a) from magnetic susceptibility measurements on bulk samples. For irregular particles and spherules, the sizes were 1.5 (0.8) μm (SS-19) and 1.9 (1.8) μm (J-02), and 0.8 (0.3) μm (SS-19) and 2.7 (2.7) μm (J-02), respectively. Larger particles were observed in the suburban site J-02 (Palpalá) because of the industrial activity in this site. One of Argentina's most important steelmaker complexes (Aceros Zapla S.A., ex "Altos Hornos Zapla") was established in Palpalá and has been working since 1945 (Peréz, 2019). Similar results, spherules ranging between 1 – 5 μm, were detected by Chaparro et al. (2013) in biomonitors living on trees

near a metallurgical factory in Tandil (Buenos Aires province, Argentina).

The analyzed AMPs were Fe-rich particles, spherules, and irregular particles (often emissions from general corrosion and brake lining system wear) emitted by traffic emissions (Lu et al., 2005; Chaparro et al., 2010; 2020; Winkler et al., 2020) and often spherules from industrial activities (Chaparro et al., 2013; Paoli et al., 2017). Fe contents ranged from 10 – 91 wt% (mean and (s.d.) values of 56 (27) wt%) for SS-19 and 6 – 97 wt% (mean and (s.d.) values of 66 (30) wt%) for J-02. Among the major elements and potentially toxic elements (PTE), Mg, Al, Si, P, S, K, Ca, Ti, Mn, Fe, Zn, Br, and Pb were determined by EDS. Iron-rich particles containing some of these PTE are shown in Figures 5c–5f.

3.3. Magnetic particle concentration and spatial distribution

The parameters κ_{is}, χ, and SIRM depend on the AMP concentration (Fig. 6). Among these parameters, the κ_{is} is used to quantify the AMP contents following the magnetite's calibration line proposed by Chaparro (2021). It is worth highlighting that the organic matter (biological tissues) has a diamagnetic matrix with contrasting magnetic values regarding ferrimagnetic AMP. According to Dearing (1999), weak negative χ values for organic matter ($\approx -9 \times 10^{-9}$ m^3kg^{-1}) are lower than for ferrimagnetic materials ($\approx 0.4 - 1.1 \times 10^{-3}$ m^3kg^{-1}). Their values varied for each site, i.e., urban, suburban, and clean sites, and between them. Mean values of κ_{is}, χ, and SIRM were found in the following order: urban sites (16.2×10^{-6} SI, 61.9×10^{-8} m^3kg^{-1}, and 4.5×10^{-3} Am^2kg^{-1}, respectively), suburban sites (13.9×10^{-6} SI, 43.9×10^{-8} m^3kg^{-1}, and 4.1×10^{-3} Am^2kg^{-1}, respectively), and clean sites ($1.6 - 2.4 \times 10^{-6}$ SI, $5.6 - 13.9 \times 10^{-8}$ m^3kg^{-1}, and $1.1 - 2.7 \times 10^{-3}$ Am^2kg^{-1}, respectively, Table S1, Supplementary Material). Among the clean sites, the lowest magnetic particle concentration values were found for site O, located in a rural area farther from cities than sites PP and TIL (Fig. 1a). These relatively higher values recorded in

Tillandsia sp. from sites PP and TIL might be related to the site's proximity to a main road. Hence, caution is recommended for the sites' selection if plant collection for transplants needs to be carried out in the future.

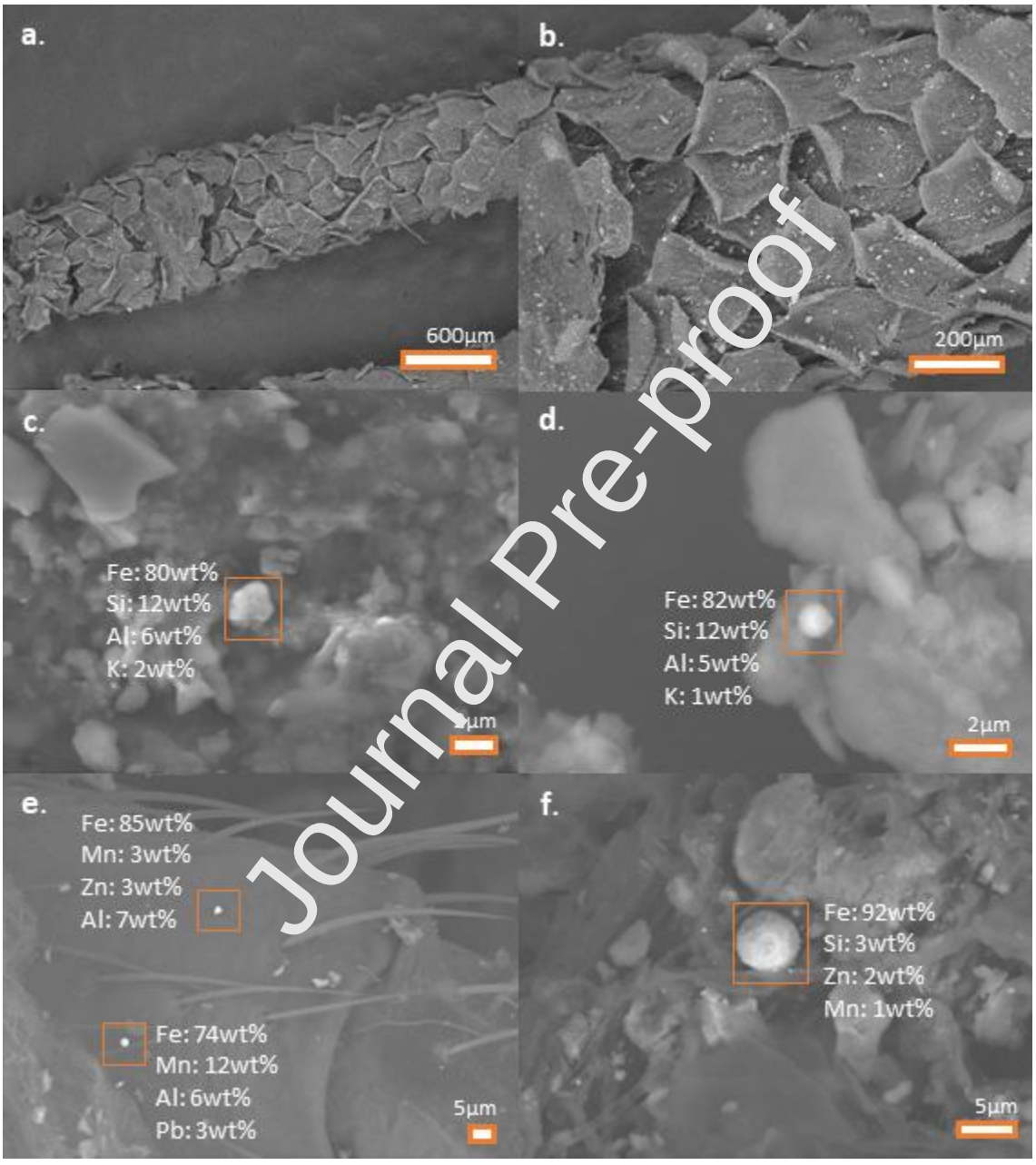

Fig. 5. SEM-EDS analysis of AMP trapped by *Tillandsia capillaris* from Jujuy. (**a**, **b**) images show trichomes covering the leaves entirely in *T. capillaris*; shiny Fe-rich particles are observed on trichomes. (**c**, **d**) urban site SS-19. (**e**, **f**) suburban site J-02.

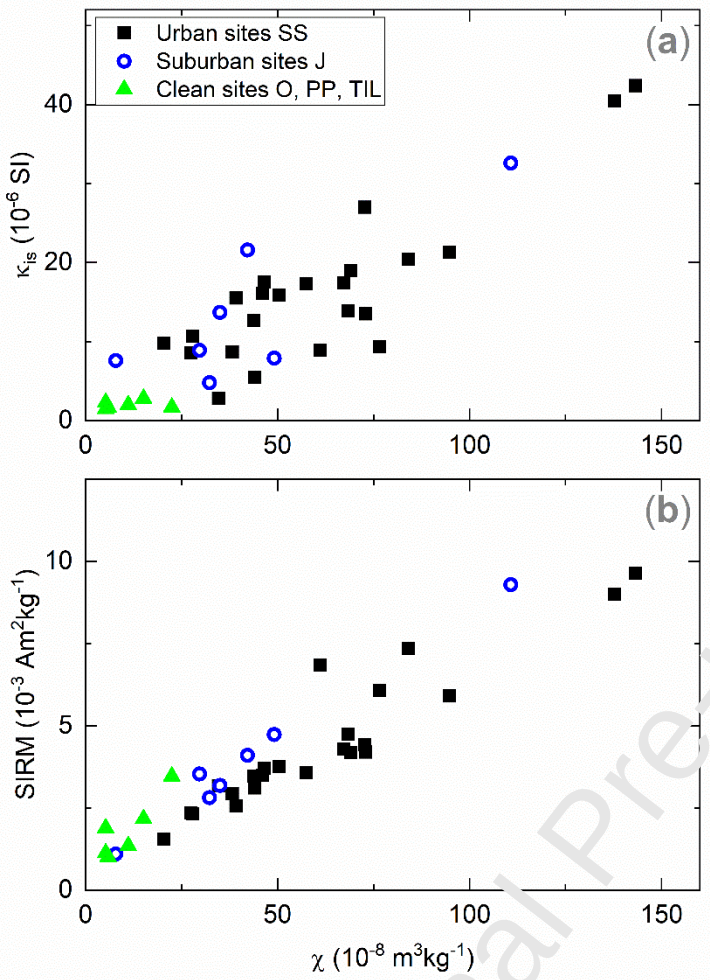

Fig. 6. Concentration-dependent magnetic parameters of AMP on *Tillandsia capillaris* samples (urban sites SS, suburban sites J and RB, and clean sites O, PP, and TIL): (**a**) *in situ* magnetic susceptibility κ_{is} and mass-specific magnetic susceptibility χ, (**b**) saturation isothermal remanent magnetization SIRM and χ.

The modeled distribution of AMP in the urban site (San Salvador de Jujuy) is represented in Figure 7, where the prediction map of κ_{is} is based on spatial autocorrelation and the Ordinary Kriging method. Among concentration-dependent magnetic parameters, the κ_{is} was chosen for modeling because it is a novel parameter for *in situ* magnetic biomonitoring. As detailed in Sect. 2.2., *in situ* magnetic susceptibility allows quantifying magnetic particles effectively and

performing repeat measurements over time because the individuals are preserved. Values of κ_{is} range between 2.8 – 42.4 $\times 10^{-6}$ SI (Table 1), and its mean (s.d.) value is 16.2 (9.4) $\times 10^{-6}$ SI (Table S1, Supplementary Material). Two outliers were observed with κ_{is} values of 40.4 and 42.4 $\times 10^{-6}$ SI, which were excluded from the construction of the geostatistical model. Moran's index test under the normality assumption was used to evaluate the spatial autocorrelation. A p-value = 0.038 was obtained; therefore, a positive autocorrelation is observed. The maximum distance between sampling points was 2138 m. The variogram was constructed considering a distance of 1000 m. The empirical variogram was fitted to an exponential model (nugget: $\tau^2 = 1 \times 10^7$, range: $\varphi = 487$, and sill: $\sigma^2 = 3.29 \times 10^7$) using weighted least squares.

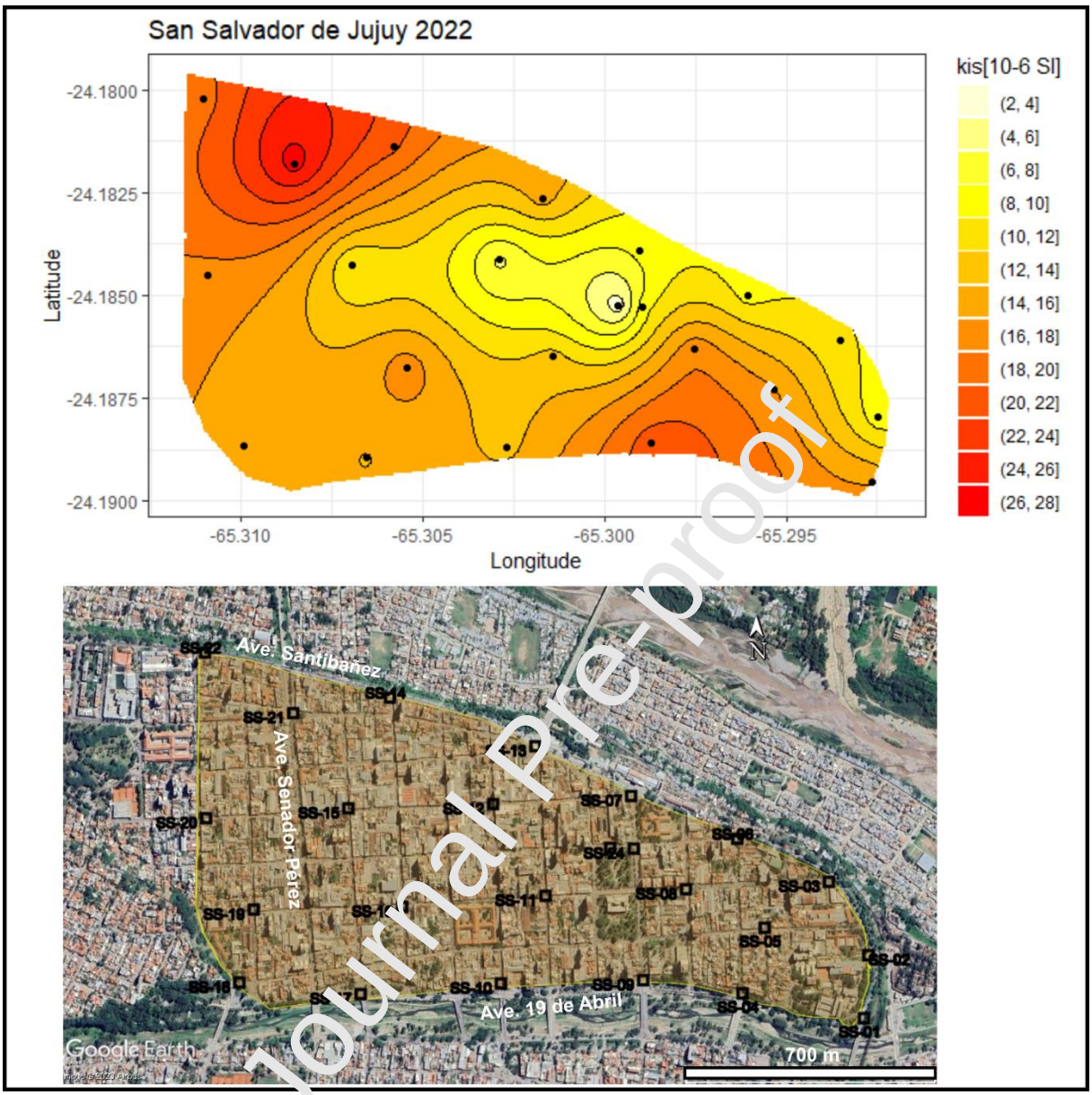

Fig. 7. (**a**) Prediction map of AMP distribution in San Salvador de Jujuy city (urban sites SS) using measurements of *in situ* magnetic susceptibility κ_{is} on native *Tillandsia capillaris*. (**b**) Sampling sites in San Salvador de Jujuy (24° 11.624'S; 65° 18.041'W), urban sites SS.

4. Discussion

4.1. Properties of airborne magnetic particles

The influence of airborne (sub)micron-sized magnetite on urban air is an increased awareness

issue (Muxworthy et al., 2022). Urban and suburban samples from Jujuy comprised magnetite with remanent coercivities (mean and (s.d.) values of H_{cr} = 38.5 (2.0) and 36.1 (2.2) mT, respectively, Table S1, Supplementary Material) associated with vehicular emissions mainly, similar to other Latin American cities, i.e., Tandil (Argentina, H_{cr} = 37.8 (1.3) mT, Chaparro et al., 2013), Querétaro (Mexico, H_{cr} = 39.4 (2.6) mT, Castañeda-Miranda et al., 2016), Valle de Aburrá (Colombia, H_{cr} = 35.0 (3.2) mT, Mejía-Echeverry et al., 2018), La Plata (Argentina, H_{cr} = 36.3 (1.6) mT, Castañeda-Miranda et al., 2018), Ushuaia (Argentina, H_{cr} = 42.4 (6.2) mT, Avalo, 2019), Mar del Plata (Argentina, H_{cr} = 38.2 8 (1.3) mT, Cénic- et al., 2021), and Medellín (Colombia, H_{cr} = 36.5 (3.1) mT, Buitrago Posada et al., 2023).

This airborne magnetite is mainly ubiquitous in all cities because of traffic emissions (Nyirő-Kósa et al., 2022) and (in some cases) industries too (Mejía-Echeverry et al., 2018). Their influence on an urban area will depend on multiple factors, such as the distance between the source and target area and meteorological conditions. In this study, fine magnetite ranging between 1 – 5 μm (urban sites) and 0.2 – 1 μm (for suburban sites, except J-02, 5 μm, Fig. 4a) is spread through the Jujuy's air. These estimated magnetic grain size ranges are based on the magnetite's calibration lines proposed by King et al. (1982) and agree with SEM observations. These airborne magnetites are not only risky for their (sub-)micron sizes (such particles can travel long distances) but also because PTEs may be adsorbed on their surface or absorbed into their structure (Kukier et al., 2003). Most of the PTEs detected by EDS have been reported in industrial and vehicle emission-related studies (Lin et al., 2005, and reference therein). Mn, Zn, Ca, Mg Ba, Fe, Co, Cd, Pb, Li, Sr, Cr, Ni, and Cu are metal-based additives detected in fuels and lubricating oils (Lim et al., 2007). PTE emissions from vehicles comprise diesel/gas-soot, general corrosion, engine wear, and brake lining system wear where Ba, Zn, Ni, Fe, Mn, C, O,

Cr, Cu, Co, Cd, Br, Pb Al, Si, Ca, S, Sb, and Mo are indicatory elements (Mosleh et al., 2004; Sanders et al., 2003; Lin et al., 2005; Maher et al., 2008). In this study, they follow the order: Fe > Si > Al > Ca > S > K > Ti, and Fe > Al > Si > Ca > Br > Mn > Zn > K > P > Mg > S > Pb > Ti for SS-19 (urban site) and J-02 (suburban site with industrial activity), respectively. As mentioned in Sect. 1, these AMPs are breathable and may adversely influence human health (Maher et al., 2016; Calderón-Garcidueñas et al., 2019; Qi et al., 2023).

4.2. Air magnetic particle pollution

Particulate matter is one of the concerning pollutants in cities considered for air quality assessment (WHO, 2021). However, high investment and maintenance costs spatially limit this monitoring coverage in urban environments (Hofman et al., 2017). Among PM, airborne magnetic particles are relevant to monitor because of their potential health risk to vulnerable populations (Gonet et al., 2021). The AMP's quantification contributes to the air quality assessment in cities, mainly where expensive PM monitoring networks are unavailable. The studied area (San Salvador de Jujuy) is one of the cities around the world where no air quality data is available. Although routine measurements (e.g., PM_1, $PM_{2.5}$, PM_{10}) are required for a complete air quality report, this work proposes a complementary methodology to sort out this deficiency, providing valuable data and a helpful approach to air particle pollution.

The *in situ* and mass-specific magnetic susceptibility were measured using different sample preparation and sensors (see Sect. 2.2). Although both are vital parameters for magnetic biomonitoring, *in situ* measurements (κ_{is}) are more convenient because plants may be preserved and monitored over time (Chaparro, 2021). Therefore, the relationship between them was examined, observing a linear trend for these data (Fig. 6a), where both parameters κ_{is} and χ are significantly correlated ($R = 0.89$, $p < 0.01$). A linear regression model with all data (urban,

suburban, and clean samples) was fitted, resulting in the following expression (2),

$\kappa_{is} = 0.268 \times \chi$ (2)

All assumptions have been adequately validated, including the intercept significantly equal to zero, the normality of errors, and the homoscedasticity of variance, establishing the model as valid. SIRM is only dependent on ferromagnetic minerals, and this parameter is significantly correlated with χ ($R = 0.94$; $p < 0.01$), as shown in Figure 6b. Thus, in this study case, the well-known magnetic susceptibility parameters, i.e., χ and κ_{is}, mainly indicate the concentration of ferrimagnetic particles or magnetite. Equation 2 establishes a linear relationship between volumetric and mass-specific magnetic susceptibility for this study and may be used for estimating χ (and SIRM) in new magnetic biomonitoring studies.

Differences in κ_{is} in the prediction map (Fig. 7a) allow identifying two main AMP accumulation zones, i.e., at the NW and SE areas ($\kappa_{is} \geq 20 \times 10^{-6}$ SI and $\geq 16 \times 10^{-6}$ SI, respectively, Fig. 7a). The NW zone (SS-14, SS-21, and SS-22) is located on Avenues Senador Pérez and Santibañez and the SE zone (SS-9 and SS-4) in Avenue 19 de Abril; they evidenced higher accumulation of AMP regarding vehicular particle emission. Conversely, the central area (SS-23 and SS-24, Fig. 7b), which comprises the historic downtown, evidences the lowest κ_{is} values ($\leq 10 \times 10^{-6}$ SI) and hence the lowest AMP contents. Notably, these AMPs on individuals of native *Tillandsia capillaris* were accumulated over their lifetime, which may cover several years of an AMP input. Thus, although the rate deposition of AMP cannot be determined for these native species, the accumulated content of AMP can be quantified following equation (1) by Chaparro (2021). The mean (s.d.) values of AMP content in clean sites (0.10 (0.02) mg) are lower than in suburban sites (0.67 (0.48) mg) and urban sites (0.78 (0.46) mg). Significant differences (at the 0.05 level) in AMP contents between (sub)urban and clean sites are observed through the Kruskal-Wallis

test (Table S2, Supplementary Material).

These recorded κ_{is} values with *T capillaris* in urban (κ_{is} = 2.8 – 42.4 × 10^{-6} SI) and suburban sites (κ_{is} = 4.8 – 32.6 × 10^{-6} SI) are lower than other available data of *in situ* magnetic biomonitoring carried out with lichens in Tandil city, Argentina (κ_{is} = 11 – 95 × 10^{-6} SI, Chaparro, 2021) and tree barks in Mar del Plata city, Argentina (κ_{is} = 2 – 202 × 10^{-6} SI, Chaparro et al., 2020). All clean sites in the present study O, PP, and TIL have lower κ_{is} values than the Tandil and Mar del Plata biomonitoring studies. However, caution for this κ_{is}-data comparison should be considered because different species may involve different AMP accumulation mechanisms. Further studies on biomonitors are needed to shed light on this issue. Among the urban and suburban sites, SS-4, SS-19 (Fig. 7a), and J-02 (Fig. 1, an industrial site at Palpalá, Table 1) evidenced the highest κ_{is} values, hence, a more significant pollution influence is expected.

Biomonitoring allows us to take advantage of natural resources, especially in urban ecosystems. *Tillandsia* spp. are distributed in several American cities, from Argentina and Chile to the south of the USA (Gouda, 2020). The occurrence of these species (and others, e.g., lichens) from the southern to northern hemisphere enables spatial-temporal measurements for establishing complementary AMP monitoring networks at a low cost. Since this species' individual is easy to collect, it offers the possibility of transplants for *in situ* magnetic biomonitoring. The methodology is sustainable because the species' individual is preserved for future κ_{is} measurements. This methodology contributes to overcoming one of the barriers in biomonitoring, i.e., the sample destruction for laboratory measurements. *In situ* magnetic biomonitoring allows quantifying AMP contents over time through exposure periods and estimating their accumulation rate. In addition, it may provide AMP data in cities and locations

where traditional air quality monitoring is absent or difficult to operate.

5. Conclusion

Like other American cities, airborne magnetic particles in San Salvador de Jujuy and Palpalá cities and their surroundings comprised magnetite mainly emitted by vehicular traffic. A suburban site at Palpalá with industrial activity also emits magnetite spherules into the air. These magnetic particles are irregular and spherical magnetites emitted by traffic and industrial emissions between 0.2 – 5 μm with potentially toxic elements (Fe > Al > Si > Ca > Br > Mn > Zn > K > P > Mg > S > Pb > Ti) absorbed or adsorbed.

The spatial distribution of airborne magnetite accumulated in native *Tillandsia capillaris* may be monitored using various concentration-dependent magnetic parameters such as κ_{is}, χ, ARM, and SIRM, which are *in situ* and at the laboratory determined. These parameters showed higher magnetic accumulation zones at the NW and the SE areas of San Salvador Jujuy's urban area, where vehicular traffic in Avenues Senador Pérez, Santibañez, and 19 de Abril seems significant. In addition, the suburban site of Palpalá also evidenced a high concentration of airborne magnetic particles due to industrial emissions from a steelmaker complex. The quantification of such particles gives significant differences in AMP contents between (sub)urban areas and clean sites, i.e., mean (s.d.) contents of AMP of 0.78 (0.46) mg for urban sites, 0.67 (0.48) mg for suburban sites, and 0.10 (0.02) mg for clean sites.

Since κ_{is} is *in situ* measured by simple contact between the sensor and the biomonitor, this parameter is preferred for airborne magnetic particle biomonitoring because plants' sampling procedures for laboratory measurements are not required, hence the preservation of *Tillandsia capillaris*' individuals. Therefore, magnetic biomonitoring may be continued over time using native individuals or transplants exposed to air particle pollution, and the AMP accumulation rate

could be estimated.

Conflict of interest

There is no conflict of interest.

Data availability

Data will be made available on request.

CRediT author statement

Marcos Chaparro: Conceptualization, Supervision, Investigation, Writing- Original draft preparation, Writing- Reviewing and Editing. **Daniela Buitrago-Posada**: Investigation, Methodology, Writing- Reviewing and Editing. **Mauro Chaparro**: Investigation, Formal analysis, Software, Visualization, Writing- Reviewing and Editing. **Daniela Molinari**: Formal analysis. **Lucas Chiavarino**: Investigation. **Brenda Alba**: Investigation. **Débora Marié**: Investigation. **Marcela Natal**: Formal analysis. **Harald Böhnel**: Writing- Reviewing and Editing. **Marcos Vaira**: Writing- Reviewing and Editing, Funding acquisition.

Acknowledgments

The authors thank UNCPBA, UNMdP, UNJu, UNAM, and CONICET for their financial support. This contribution was partially supported by projects ImpaCT.AR–Desafio N°38 (Ministerio de Ciencia, Tecnología e Innovación) and P-UE-2017-22920170100004CO (CONICET). The authors thank Ing. J. Escalante and Dr. Marina Vega (Centro de Geociencias, UNAM, México), and O. Peinado (INECOA, UNJu-CONICET, Jujuy, Argentina) for help during fieldwork. The authors thank the Editor, Melina Macouin, and two anonymous reviewers whose comments significantly improved this manuscript. The authors also thank Secretaría Provincial de Biodiversidad y Desarrollo Sustentable of the Ministerio de Ambiente y Cambio Climático of Jujuy Province for providing us with the research permits (Resol. 040/2017-SB).

References

Avalo, E.M., 2019. El uso de las especies vegetales endémicas de Ushuaia en biomonitoreos magnéticos de contaminantes atmosféricos. Master of Science Thesis, in Spanish. Universidad Nacional de la Provincia de Buenos Aires, p. 95. https://www.ridaa.unicen.edu.ar/handle/123456789/2638. Accessed 30 June 2023.

Brauer, M., Hoek, G., Van Vliet, P., Meliefste, K., Fischer, P.H., Wijga, A., Koopman, L.P., Neijens, H., Gerritsen, J., Kerkhof, M., Heinrich, J., Bellander, T., Brunekreef, B., 2002. Air pollution from traffic and the development of respiratory infections and asthmatic and allergic symptoms in children. Am. J. Respir. Crit. Care Med. https://doi.org/10.1164/rccm.200108-007OC

Buitrago Posada, D., Chaparro, M.A.E., 2022. *In situ* magnetic biomonitoring using transplants of *Tillandsia capillaris* (bromeleacea) in two midsize Argentinian cities. 9th International Workshop on Biomonitoring of Atmospheric Pollution. Napoli, Italy. Book Abstracts, 53. https://biomap9.azuleon.org/welcome

Buitrago Posada, D., Chaparro, M.A.E., Duque-Trujillo, J.F., 2023. Magnetic Assessment of Transplanted *Tillandsia* spp.: Biomonitors of Air Particulate Matter for High Rainfall Environments. Atmosphere 14, 213. https://doi.org/10.3390/atmos14020213

Calderón-Garcidueñas, L., González-Maciel, A., Mukherjee, P.S., Reynoso-Robles, R., Pérez-Guillé, B., Gayosso-Chávez, C., Torres-Jardón, R., Cross, J.V., Ahmed, I.A.M., Karloukovski, V.V., Maher, B.A., 2019. Combustion- and friction-derived magnetic air pollution nanoparticles in human hearts. Environ. Res. 176, 108567. https://doi.org/10.1016/j.envres.2019.108567

Castañeda-Miranda, A.G., Chaparro, M.A.E., Chaparro, M.A.E., Böhnel, H.N., 2016. Magnetic properties of *Tillandsia recurvata* L. and its use for biomonitoring a Mexican metropolitan area. Ecol. Indic. 60, 125-136. http://dx.doi.org/10.1016/j.ecolind.2015.06.025

Castañeda-Miranda, A.G., Chaparro, M.A.E., Marié, D.C., Chaparro, M.A.E., 2018. Uso de la epífita *Tillandsia recurvata* para biomonitoreo magnético de contaminación atmosférica en La Plata, Argentina [Use of *Tillandsia recurvata* for magnetic biomonitoring of atmospheric pollution in La

Plata, Argentina]. Geos 38 (1), 79-80.

Censo nacional de población, hogares y viviendas 2022: resultados provisionales / 1a ed. - Ciudad Autónoma de Buenos Aires : Instituto Nacional de Estadística y Censos - INDEC, 2023. Libro digital, PDF - (Censo nacional de población, hogares y viviendas 2022). ISBN 978-950-896-633-9. https://www.censo.gob.ar/index.php/datos_provisionales/. Accessed 26 April 2023.

Chaparro, M.A.E., 2021. Airborne particle accumulation and loss in pollution-tolerant lichens and its magnetic quantification. Environ. Pollut. 288, 117807. https://doi.org/10.1016/J.ENVPOL.2021.117807

Chaparro, M.A.E., Marié, D.C., Gogorza, C.S.G., Navas, A., Sinito, A.M., 2010. Magnetic studies and scanning electron microscopy X-ray energy dispersive spectroscopy analyses of road sediments, soils, and vehicle-derived emissions. Stud. Geophys. Geod. 54 (4), 633-650. https://doi.org/10.1007/s11200-010-0038-2

Chaparro, M.A.E., Lavornia, J.M., Chaparro, M.A.E., Sinito, A.M., 2013. Biomonitors of urban air pollution: magnetic studies and SEM observations of corticolous foliose and microfoliose lichens and their suitability for magnetic monitoring. Environ. Pollut. 172, 61–69. https://doi.org/10.1016/j.envpol.2012.08.006

Chaparro, M.A.E., Chaparro, M.A.E., Castañeda Miranda, A.G., Marié, D.C., Gargiulo, J.D., Lavornia, J.M., Natal, M., Böhnel, H.N., 2020. Fine air pollution particles trapped by street tree barks: *in situ* magnetic biomonitoring. Environ. Pollut. 226 (1): 115229, https://doi.org/10.1016/j.envpol.2020.115229

Conover, W.J., 1999. Practical Nonparametric Statistics. 3rd ed.; John Wiley & Sons Inc.: New York, pp. 608.

Dearing, J., 1999. Environmental magnetic susceptibility. Using the Bartington MS2 System. 2nd edition, Chi Publishing: Kenilworth, 54 pp.

Dunlop, D., 2002. Theory and application of the Day plot (*Mrs*/*Ms* versus *Hcr*/*Hc*) 1. Theoretical curves and tests using titanomagnetite data. J. Geophys. Res. 107(B3), https://doi.org/10.1029/2001JB000486

Escalante, J.E., Böhnel, H.N., 2011. Diseño y Construcción de una Balanza de Curie [Design and construction of a Curie Balance]. Geos 31(1), 63.

Gómez, R.Q., Chaparro, M.A.E., Chaparro, M.A.E., Castañeda-Miranda, A.G., Marié, D.C., Gargiulo, J.D., Böhnel, H.N., 2021. Magnetic Biomonitoring Using Native Lichens: Spatial Distribution of Traffic-Derived Particles. Water Air Soil Pollut. 232, 124. https://doi.org/10.1007/s11270-021-05047-w

Gonet, T., Maher, B.A., Kukutschova, J., 2021a. Source apportionment of magnetite particles in roadside airborne particulate matter. Sci. Total Environ. 752. https://doi.org/10.1016/j.scitotenv.2020.141828

Gouda, E.J., 2020. Tillandsia BROMELIACEAE. In *Monocotyledons* (pp. 1107–1164). Springer Berlin Heidelberg. https://doi.org/10.1007/978-3-662-56486-8_96

Hofman, J., Maher, B.A., Muxworthy, A.R., Wuyts, K., Castanheiro, A., Samson, R., 2017. Biomagnetic Monitoring of Atmospheric Pollution: A Review of Magnetic Signatures from Biological Sensors. Environmental Science & Technology 51 (12), 6648-6664. https://doi.org/10.1021/acs.est.7b00832

Hrouda, F., 2011. Models of frequency-dependent susceptibility of rocks and soils revisited and broadened. Geophys. J. Int. 187(3), 1259–1269, https://doi.org/10.1111/j.1365-246X.2011.05227.x

Karagulian, F., Dora, C., Belis, C.A., Dora, C.A.C., Prüss-Ustün, A., Bonjour, S., Adair-Rohani, H., Amann, M., 2015. Contributions to cities' ambient particulate matter (PM): a systematic review of local source contributions at global level. Atm. Environ. 120, 475-483. https://doi.org/10.1016/j.atmosenv.2015.08.087

King, J., Banerjee, S.K., Marvin, J., Özdemir, Ö., 1982. A comparison of different magnetic methods for determining the relative grain size of magnetite in natural materials: Some results from lake sediments. Earth Planet. Sci. Lett. 59, 404-419. https://doi.org/10.1016/0012-821X(82)90142-X.

Kletetschka, G., Bazala, R., Takáč, M., Svecova, E., 2021. Magnetic domains oscillation in the brain with neurodegenerative disease. Sci. Rep. 11, 714. https://doi.org/10.1038/s41598-020-80212-5

Kukier, U., Fauziah, I.C., Summer, M.E., Miller, W.P., 2003. Composition and element solubility of magnetic and non-magnetic fly ash fractions. Environ. Pollut. 123, 255-266.

https://doi.org/10.1016/S0269-7491(02)00376-7

Lehndorff, E., Urbat, M., Schwark, L., 2006. Accumulation histories of magnetic particles on pine needles as function of air quality. Atmos. Environ. https://doi.org/10.1016/j.atmos env.2006.06.008

Lim, M.C.H., Ayodo, G.A., Morawska, L., Ristovski, Z.D., Jayaratne, E.R., 2007. The effects of fuel characteristics and engine operating conditions on the elemental composition of emissions from duty diesel buses. Fuel, 86, 1831-1839. https://doi.org/10.1016/j.fuel.2006.11.025

Lin, C.-C., Chen, S.-J., Huang, K.L., 2005. Characteristics of metals in nano/ultrafine/fine/coarse particles collected beside a heavily trafficked road. Environ. Sci. Technol., 39, 8113-8122. https://doi.org/10.1021/es048182a

Liu, Q., Roberts, A.P., Torrent, J., Horng, C.-S., Larrasoaña, J.C., 2007. What do the HIRM and S-ratio really measure in environmental magnetism? Geochem. Geophys. Geosyst. 8, Q09011, https://doi.org/10.1029/2007GC001717

Lu, S.-G., Bai, S.-Q., Cai, J.-B., Xu, C., 2005. Magnetic properties and heavy metal contents of automobile emission particulates. J. Zhejiang Univ. Sci. 6B(8), 731-735. https://doi.org/10.1631/jzus.2005.B0731

Maher B.A., Moore C. and Matzka J., 2008. Spatial variation in vehicle-derived metal pollution identified by magnetic and elemental analysis of roadside tree leaves. Atmos. Environ., 42, 364-373. https://doi.org/10.1016/j.atmosenv.2007.09.013.

Maher, B.A., Ahmed, I.A.M., Karloukovski, V., MacLaren, D.A., Foulds, P.G., Allsop, D., Mann, D.M.A., Torres-Jardón, R., Calderon-Garciduenas, L., 2016. Magnetite pollution nanoparticles in the human brain. Proc. Natl. Acad. Sci. USA 113, 10797-10801. https://doi.org/10.1073/pnas.1605941113

Marié, D.C., Chaparro, M.A.E., Lavornia J.M., Sinito, A.M., Castañeda Miranda, A.G., Gargiulo, J.D., Chaparro, M.A.E., Böhnel, H.N., 2018. Atmospheric pollution assessed by *in situ* measurement of magnetic susceptibility on lichens. Ecol. Indic. 95, 831-840. https://doi.org/10.1016/j.ecolind.2018.08.029

Marié, D.C., Chaparro, M.A.E., Sinito, A.M., Lavat, A., 2020. Magnetic biomonitoring of airborne

particles using lichen transplants over controlled exposure periods. SN Appl. Sci. 2, 104. https://doi.org/10.1007/s42452-019-1905-2

Mejía-Echeverry, D., Chaparro, M.A.E., Duque-Trujillo, J.F., Chaparro, M.A.E., Castañeda-Miranda, A.G., 2018. Magnetic biomonitoring of air pollution in a tropical valley using a *Tillandsia* sp. Atmosphere 9, 283. https://doi.org/10.3390/atmos9070000

Mosleh, M., Blau, P.J., Dumitrescu, D., 2004. Characteristics and morphology of wear particles from laboratory testing of disk brake materials. Wear, 256, 1128-1134. https://doi.org/10.1016/j.wear.2003.07.007

Muxworthy, A.R., Lam, C., Green, D., Cowan, A., Maher, B.A., Gonet, T., 2022. Magnetic characterisation of London's airborne nanoparticulate matter. Atm. Environ. 287, 119292. https://doi.org/10.1016/j.atmosenv.2022.119292

Nyirő-Kósa, I., Ahmad, F., Hoffer, A., Pósfai, M., 2022. Nanoscale physical and chemical properties of individual airborne magnetic particles from vehicle emissions. Atm. Environ. X, 15, 100181. https://doi.org/10.1016/j.aeaoa.2022.100181

Palmgren, F., Waahlin, P., Kildesó, J., Afshari, A., Fogh, C.L., 2003. Characterization of particle emissions from the driving car fleet and the contribution to ambient and indoor particle concentrations. Phys. Chem. Earth 28, 327-334. https://doi.org/10.1016/S1474-7065(03)00053-6

Paoli, L., Winkler, A., Guttová, A., Sagnotti, A., Grassi, A., Lackovičová, A., Senko, D., Loppi, S., 2017. Magnetic properties and element concentrations in lichens exposed to airborne pollutants released during cement production. Environ. Sci. Pollut. Res. 24 (13), 12063-12080. https://doi.org/10.1007/s11356-016-6203-6

Pérez, J.R., 2019. "Problemática Ambiental de Palpalá", Cuadernos de Ingeniería, (2), pp. 68-83. https://revistas.ucasal.edu.ar/index.php/CI/article/view/188. Accessed 14 August 2023.

Peters, C., Dekkers., M., 2003. Selected room temperature magnetic parameters as a function of mineralogy, concentration and grain size. Phys. Chem. Earth 28, 659-667. https://doi.org/10.1016/S1474-7065(03)00120-7

Pope, C.A., Dockery, D.W., 2006. Health effects of fine particulate air pollution: lines that connect. J. Air Waste Manage. Assoc. 56, 709-742. https://doi.org/10.1080/10473289.2006.10464485

Qi, Y., Chen, Y., Xia, T., Lynch, I., Liu, S., 2023. Extra-Pulmonary Translocation of Exogenous Ambient Nanoparticles in the Human Body. ACS Nano 17 (1), 12-19. https://doi.org/10.1021/acsnano.2c09299

R Core Team, 2022. R: A language and environment for statistical computing. R Foundation for Statistical Computing, Vienna, Austria. URL https://www.R-project.org/. Accessed 3 July 2023.

Salo, H., Bucko, M.S, Vaahtovuo, E., Limo, J., Mäkinen, J., Pesonen, L.J., 2012. Biomonitoring of air pollution in SW Finland by magnetic and chemical measurements of moss bags and lichens. J. Geoch. Expl. 115 69-81. https:// doi.org/10.1016/j.gexplo.2012.02.009

Sanders, P., Xu, N., Dalka, T., Maricq, M.M., 2003. Airborne brake wear debris: size distributions, composition, and a comparison of dynamometer and vehicle test. Environ. Sci. Technol. 37, 4060-4069. https://doi.org/10.1021/es034145s

Servicio Meteorólogico Nacional, 2023. Mean meteorological data for 1991–2020. https://www.smn.gob.ar/estadisticas. Accessed 26 April 2023.

Song, Y., Wang, X., Maher, B.A., Li, F., Xu, C., Liu, X., Sun X., Zhang, Z., 2017. Reprint of: The spatial-temporal characteristics and health impacts of ambient fine particulate matter in China. J Clean Prod. 163, Supplement, S352-S358. https://doi.org/10.1016/j.jclepro.2017.05.145

Vuković, G., Aničić Urošević, M., Tomašević, M., Samson, R., Popović, A., 2015. Biomagnetic monitoring of urban air pollution using moss bags (*Sphagnum girgensohnii*). Ecol. Indic. 52, 40-47. https://doi.org/10.1016/j.ecolind.2014.11.018

Torres, G.R., Pereira, E. de los A., 2018. Monitoring of the airborne pollen Diversity in the urban area of San Salvador de Jujuy, Argentina. Biodiversity Int. J. 2(1): 00046. https://doi.org/10.15406/bij.2018.02.00046

World Health Organization, 2021. WHO global air quality guidelines: particulate matter (PM2.5 and PM10), ozone, nitrogen dioxide, sulfur dioxide and carbon monoxide. World Health Organization. https://apps.who.int/iris/handle/10665/345329

Winkler, A., Contardo, T., Vannini, A., Sorbo, S., Basile, A., Loppi, S., 2020. Magnetic emissions from brake wear are the major source of airborne particulate matter bioaccumulated by lichens exposed in Milan (Italy). App. Sci. 10, 2073. https://doi.org/10.3390/app10062073

Table captions

Table 1. Magnetic measurements of *Tillandsia capillaris* samples from the study area (Jujuy, NW Argentina).

Table S1. Descriptive statistics of magnetic measurements of *Tillandsia capillaris* samples from Jujuy, NW Argentina. Results are detailed for urban sites (sites SS), suburban sites (sites J and RB), and clean sites (sites O, PP, and TIL).

Table S2. Kruskal-Wallis test of *Tillandsia capillaris* samples from urban, suburban, and clean sites. Statistical differences in median values of χ_{ARM}/χ, ARM/SIRM, SIRM/χ, and AMP contents are indicated. YES indicates that differences are significant at the 0.05 level.

Figure captions

Fig. 1. Sampling sites in northwestern Argentina. (**a**) San Salvador de Jujuy (urban sites SS, 24° 11.624'S; 65° 18.041'W), Alto Comedero, Río Blanco, and Palpalá (suburban sites J and RB) and clean areas (sites O, PP, and TIL). (**b**) Individuals of *Tillandsia capillaris*; (**c**) Collection of samples in urban sites SS.

Fig. 2. *In situ* magnetic susceptibility measurements (κ_{is}) using the protocol proposed by Chaparro (2021) and Buitrago Posada & Chaparro (2022). Ten readings were performed by contact between a high-resolution range portable meter SM 30 (ZH Instruments Ltd.) and a Petri plastic dish where the plant is pressed with a block of wood to increase the plant's surface contact (PWM). κ_{is} readings at the laboratory (**a**) and inside a car (**b**) close to the sampling site.

Fig. 3. Thermomagnetic measurements of *Tillandsia capillaris* samples from the Jujuy area

(urban sites SS, suburban sites J and RB, and clean sites O and PP). Magnetization (M) was normalized by magnetization at room temperature (M_{RT}); its changes with temperature were recorded for heating (heat.) and cooling (cool.) runs.

Fig. 4. Particle size-dependent magnetic parameters of AMP on *Tillandsia capillaris* samples (urban sites SS, suburban sites J and RB, and clean sites O, PP, and TIL) and dust samples (P-A at downtown sites SS, and P-T at Palpalá): (**a**) parameters χ_{ARM} and χ are represented, the indicated samples SS-19 and J-02 were observed by SEM-EDS; (**b**) the anhysteretic ratio χ_{ARM}/χ, calibration lines are based on data reported by King et al. (1982), (**c**) parameters from magnetic hysteresis measurements, i.e., M_{rs}/M_s and H_{cr}/H_c, and mixing lines for SD-MD, SD-SP, and SP-PSD (Dunlop, 2002); and (**d**) magnetic hysteresis measurements of samples SS-10 and J-02 are also represented.

Fig. 5. SEM-EDS analysis of AMP trapped by *Tillandsia capillaris* from Jujuy. (**a**, **b**) images show trichomes covering the leaves entirely in *T. capillaris*; shining Fe-rich particles are observed on the surface. (**c**, **d**) urban site SS-19. (**e**, **f**) suburban site J-02.

Fig. 6. Concentration-dependent magnetic parameters of AMP on *Tillandsia capillaris* samples (urban sites SS, suburban sites J and RB, and clean sites O, PP, and TIL): (**a**) *in situ* magnetic susceptibility κ_{is} and mass-specific magnetic susceptibility χ, (**b**) saturation isothermal remanent magnetization SIRM and χ.

Fig. 7. (**a**) Prediction map of AMP distribution in San Salvador de Jujuy city (urban sites SS) using measurements of *in situ* magnetic susceptibility κ_{is} on native *Tillandsia capillaris*. (**b**) Sampling sites in San Salvador de Jujuy (24° 11.624’S; 65° 18.041’W), urban sites SS.

Declaration of interests

☒ The authors declare that they have no known competing financial interests or personal relationships that could have appeared to influence the work reported in this paper.

☐The authors declare the following financial interests/personal relationships which may be considered as potential competing interests:

Graphical abstract

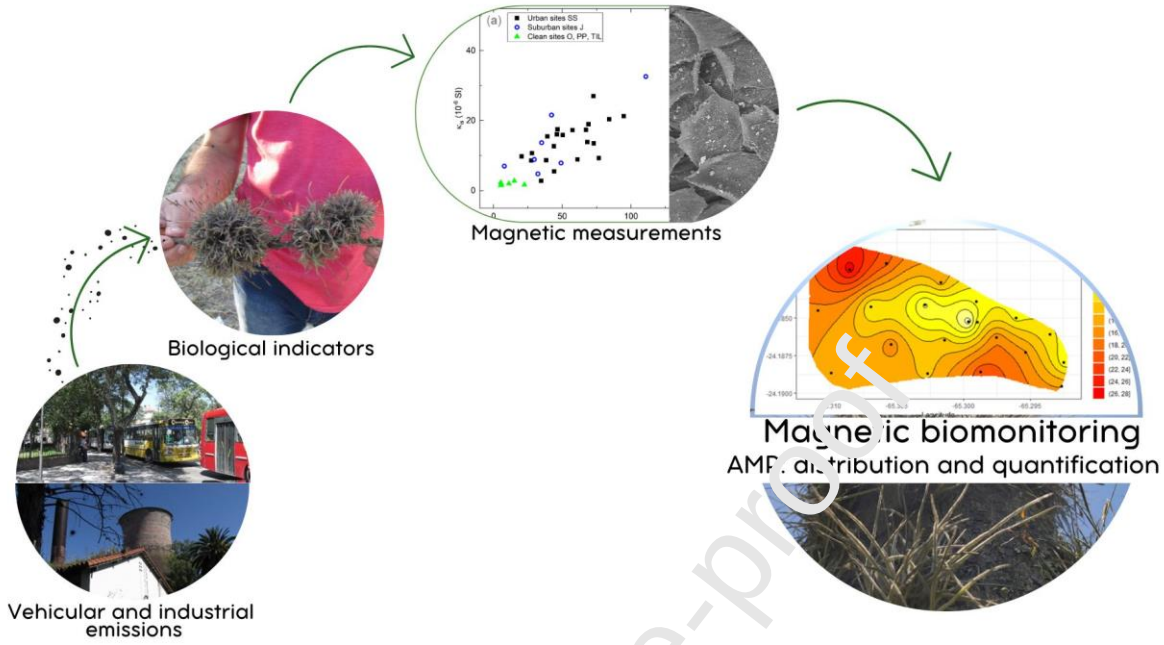

Highlights

Tillandsia capillaris is efficient for monitoring airborne micron-sized particles

Airborne magnetic particle AMP contents here are ordered as urban>suburban>clean sites

In situ magnetic susceptibility of biomonitors allows the AMP quantification